Jpn. J. Appl. Phys. Vol. 38 (1999) pp. 674–680
Part 1, No. 2A, February 1999

Time-resolved Photoluminescence and Carrier Dynamics in Vertically-coupled Self-assembled Quantum Dots

I. GONTIJO, G. S. BULLER, J. S. MASSA, A. C. WALKER, S. V. ZAITSEV[1], N. Yu. GORDEEV[1], V. M. USTINOV and P. S. KOP'EV[1]

Department of Physics, Heriot-Watt University, Edinburgh EH14 4AS, Scotland
[1]*A. F. Ioffe Physical-Technical Institute, St. Petersburg, 194021, Russia*

(Received September 14, 1998; accepted for publication November 6, 1998)

The relaxation mechanisms of an array of 10 vertically coupled layers of InGaAs/AlGaAs quantum dots were studied by time-resolved photoluminescence. Both resonant and non-resonant excitation were employed and the photoluminescence (PL) intensity in the non-resonant case is a factor of 200 larger than the intensity with resonant excitation. The results obtained in the non-resonant pumping experiment were analysed with a rate equation model. It was found that the PL decay time increases rapidly with the wavelength of detection. Large carrier capture cross-sections [$(2.5 \pm 0.9) \times 10^{-5}$ cm^3/s] were deduced, resulting in a capture time of 1 ps for a carrier concentration of 4×10^{16} cm^{-3}. A very fast PL risetime was observed with resonant pumping, ruling out a phonon bottleneck effect in these samples. The decay times at a given wavelength are always shorter for resonant than for non-resonant excitation and their difference increases rapidly with wavelength. This is interpreted in terms of a state filling effect for the non-resonant case.

KEYWORDS: III–V semiconductors, quantum dots, carrier dynamics, photoluminescence, diode lasers

1. Introduction

The study of the excess carrier relaxation mechanisms in quantum dots (QDs) is of vital importance for a more complete understanding of devices based on these structures.[1)] The 3D quantum confinement in QDs can lead to severe restrictions in the possible energy relaxation mechanisms available to electrons and holes. It has been shown theoretically that these structures can consequently have very long relaxation times, compared to 2D or bulk materials.[2)] In order to conserve both energy and momentum, the resulting selection rules establish that there is an efficient relaxation mechanism only when the separation between energy levels is equal to the LO phonon energy in the material. If this condition is not met, the carriers cannot relax efficiently to the ground state, with a consequent poor photoluminescence efficiency. This effect has become known as the phonon bottleneck effect.[2)]

Many other relaxation mechanisms have been suggested, which could alleviate the problem of slow carrier relaxation in these materials. Multiphonon effects, with the emission of an LO phonon and the absorption or emission of an LA phonon to preserve the energy balance could produce relaxation times of the order of a few picoseconds.[3)] Carrier-carrier scattering, in an Auger-like process has also been proposed[4,5)] and shown to play a significant role.

In addition, other effects that can take place in quantum dots are band filling and inhomogeneous broadening of photoluminescence (PL) signals due to size fluctuations.[6)] In a single quantum well embedded in an optical waveguide, band filling can be easily seen, even with modest pump powers produced by a semiconductor laser.[7)] It is expected that this effect should be even stronger in quantum dots, due to the reduced density of states.

The experimental results reported in the literature concerning photoluminescence efficiency and relaxation mechanisms in quantum dots have been contradictory. The poor luminescence efficiency of quantum cylinders, fabricated from quantum well material by electron beam lithography and dry etching techniques, was explained as a result of the selection rules imposed by the reduced dimensionality (the phonon bottleneck effect). Later reports of experiments in self assembled quantum dots and in spherical CdSe nanocrystals both confirmed[8,9)] and denied[4,5)] the severity of this problem. At present, there is no consensus as to what relaxation mechanisms are active in quantum dots and as to what conditions are sufficient for them to dominate the relaxation process.

A time-resolved photoluminescence (TRPL) study of 10 layers of InGaAs/AlGaAs vertically-coupled self-assembled quantum dots (VECODs) is reported below. Both carrier capture and their subsequent relaxation were investigated. These VECOD structures have a number of properties which make them more attractive for laser diode fabrication than a single layer of quantum dots. The threshold current density (J_{th}) in a VECOD laser decreases when the number N of QD layers is increased.[10)] For InGaAs QDs, it decreases by one order of magnitude, from 950 A/cm^2 for $N = 1$, to 98 A/cm^2, for $N = 10$. In addition, the range of threshold current stability for VECOD laser diodes embedded in an external quantum well has been shown to extend up to room temperature[10)] and these devices exhibited an internal quantum efficiency as high as 70%.

2. Experiments and Analysis of Results

The vertically-coupled, self-assembled QDs used in this study consisted of 10 layers of InGaAs QDs separated by AlGaAs barriers. Doped layers above and below the QDs formed a p-n junction. Quantum dot lasers fabricated from this material structure produced threshold current densities as low as 60 A/cm^2, at room temperature.[11)] The samples were grown by molecular beam epitaxy on (100) n-type GaAs substrates. Firstly, a 0.2 μm GaAs (Si-doped, 3×10^{18} cm^{-3}) buffer layer was grown, followed by a graded AlGaAs layer (from 0 to 0.45 Al) of the same thickness and doping. An $Al_{0.45}Ga_{0.55}As$ (Si-doped 1.5×10^{18} cm^{-3}) lower cladding layer 1.5 μm thick was then grown, followed by a 0.15 μm superlattice layer (undoped), composed of (10 Å GaAs/20 Å $Al_{0.2}Ga_{0.8}As$) $\times$ 50. Ten periods of (undoped) quantum dots/barriers were then grown with composition and thick-

ness of (12 Å $In_{0.5}Ga_{0.5}As$/50 Å $Al_{0.15}Ga_{0.85}As$). Above the quantum dot layers a second, identical superlattice layer was grown, followed by an $Al_{0.45}Ga_{0.55}As$ layer (Be-doped $8 \times 10^{18}\,cm^{-3}$) of thickness 1.5 μm. Another graded layer (from 0.45 to 0) of AlGaAs (Be-doped $3.5 \times 10^{18}\,cm^{-3}$) 0.2 μm thick was grown and the structure was completed by a 0.6 μm GaAs contact capping layer (Be-doped $3.5 \times 10^{18}\,cm^{-3}$). The ten periods of InGaAs/AlGaAs QDs and barriers were grown at 485°C and all the other layers were grown at 600°C. Figure 1 shows a transmission electron micrograph (TEM) image of the quantum dot laser structure cross section. The vertical alignment of the quantum dots (due to strain-induced nucleation), the thin wetting layer surrounding the dots and the superlattices above and below the quantum dots region are all clearly evident. From other TEM images,[12] which show a much larger area of the sample, it was found that on average, there are 8.6×10^{10} dots/cm^2 in the sample, with an in-plane dot separation of 34 nm. Electroluminescence and cw PL were performed at 77 K on these samples and three distinct emission peaks have been obtained, at 910, 940 and 980 nm, as shown in Fig. 2. These cw measurements were useful to select the wavelengths of interest for the time-resolved studies. The first thing to notice in this spectrum is that the three peaks overlap to a great extent. This is caused by inhomogeneous broadening (caused by QD size fluctuations generated during growth, which are still unavoidable) and thermal broadening.

Due to the material composition and the peak wavelengths above, it is suggested that the whole spectrum of Fig. 2 originates in the VECODs, as opposed to the wetting layer. The InGaAs wetting layer (WL) forms a very narrow quantum well, only one or two monolayers thick (see Fig. 1), because part of the InGaAs material deposited, which is only 1.2 nm in total thickness, goes into the formation of the QDs. The barriers of the WL quantum well are formed by the $Al_{0.15}Ga_{0.85}As$ matrix, which has a bandgap of $E_g = 1.611$ eV and corresponding wavelength of $\lambda_g = 771$ nm. As this QW is so narrow, its bound energy level must be very close to its barrier, giving therefore a very short wavelength, probably somewhere between 771 and 800 nm.

In general, fast TRPL measurements are performed with solid state lasers producing short pulses and photomultipliers or streak cameras used for the detection of the luminescence. The TRPL system employed for this study has unique features which makes it very attractive for the routine investigation of carrier recombination mechanisms in semiconductors.[13] Specifically, Q-switched semiconductor lasers producing pulses of about 20 ps at a repetition rate of 1 MHz are used as the excitation source with Si single-photon avalanche diodes (Si-SPADs) for the detection of the luminescence.[14] Besides the general advantages found in using solid-state devices when compared with photomultipliers, Si-SPADS exhibit superior photon detection eficiency and faster and cleaner time response.[15,16] The small active area (~7 μm diameter), presents a considerable advantage in these applications, making possible high spatial resolution measurements with low sensistivity to spurious back scatter. The width of the instrumental response (FWHM) in our TRPL system is around 80 ps. The whole instrument is mounted on a microscope and has been described elsewhere.[13]

All TRPL measurements described below were performed at 77 K. As the material in which the QDs are embedded in

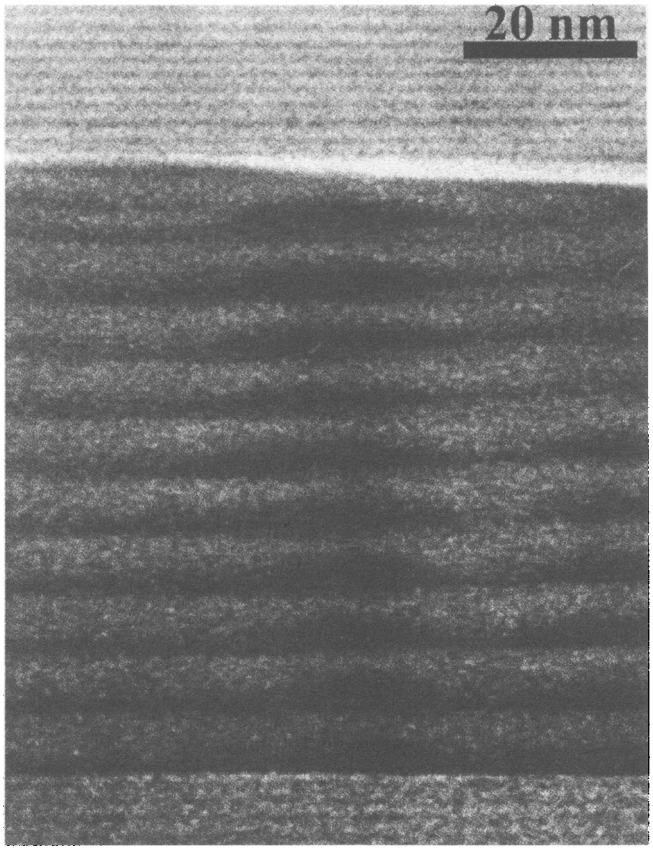

Fig. 1. TEM micrograph of the sample cross-section. The ten QD layers, barriers, wetting layers and the superlattices above and below the QDs are all clearly evident.

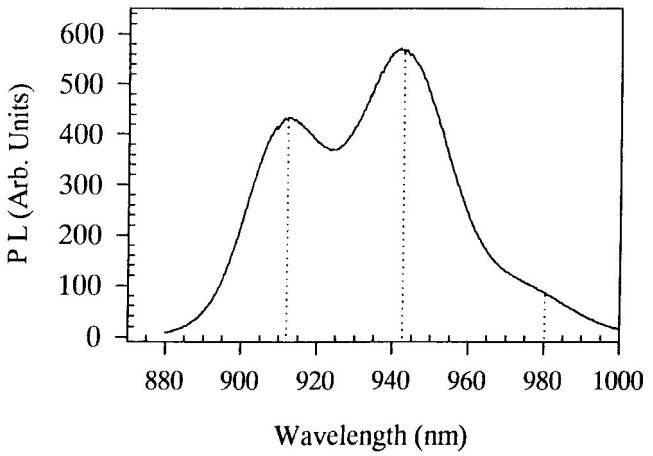

Fig. 2. VECODs CW PL spectrum, obtained with 514 nm pump wavelength.

is an actual laser structure, the top layers are highly doped. To lower the free-carrier absorption of the excitation pulse, 1.5 μm was etched from the top layers. This still left about 0.8 μm of doped material above the QDs, (apart from the nominally undoped superlattice). Such a thick layer was left above the dots to ensure that they were not damaged by the etching process.

Both resonant and non-resonant light can be used to excite the quantum dot structure. Firstly, the wavelength can be chosen so that it is longer than the absorption edge of the barriers and the wetting layer. In this case, these layers are transparent

to the excitation and only the quantum dot layers are excited by the laser pulse. This is the "resonant excitation" condition. In the "non-resonant" case the laser wavelength is chosen so that it excites all the layers, including the barriers, the wetting layer and the dots. Due to the small in-plane QD coverage, which is around 10%, most of the light will be absorbed by the other layers. Nonetheless the carriers thus generated can be captured by the QDs. The non-resonant pumping condition can excite much higher numbers of carriers, resulting in larger PL signals. However, the carrier dynamics are further complicated by effects outside the QDs, such as local carrier drift and diffusion (in the barriers) and the rate of carrier capture by the QDs.

In our resonant pumping experiment, excitation was by an 870 nm (1.428 eV) semiconductor laser, which produced 20 ps pulses and was focussed to a 2 μm spot diameter on the sample surface. This wavelength was chosen so that the wetting layer is transparent to the laser pulses. As discussed previously, the energy level of the wetting layer is close to 1.6 eV. Therefore, only the VECODs will be resonantly pumped in this experiment. The laser energy, measured at the sample plane, was 0.5 pJ/pulse. In this case, carriers were generated inside the dots only and carrier drift, diffusion and capture by the dots need not be considered.

As the pumping and detection wavelengths were very close, there is a strong possibility of laser light reflected by the sample being detected by the Si-SPAD, thus affecting the TRPL measurements. Also, the laser might have produced a small amount of spontaneous emission at the detection wavelength and similarly affected the measurements. To avoid these problems, an interference filter centred at 870 nm, with a bandpass of 10 nm was mounted at the laser output, to block any spontaneous emission at other wavelengths. A second interference filter centred at 890 nm (10 nm bandpass) was mounted in front of the detector to select the PL only at this wavelength and to block unwanted laser reflections reaching the detector. Polarising elements were also used to further discriminate against direct detection of the laser excite pulse. For PL measurements at longer wavelengths, other interference filters were used in front of the detector, in place of the 890 nm filter.

Time-resolved photoluminescence measurements using resonant excitation were performed as a function of wavelength and Fig. 3 shows the PL decay at the detection wavelength of 900 nm. Three of the curves in the figure are the instrumental response $I(t)$, the measured (resonant) PL decay $M(t)$ and the best multi-exponential curve fitting the experimental result. The TRPL decay obtained by non-resonant pumping (to be described below) is also shown for comparison. The instrumental response is limited by the Si-SPAD detector and has a FWHM of 72 ps and a FWTM (Full Width at Tenth Maximum) of 364 ps. In these measurements, it is worth noting that the risetime of the measured PL signals is very fast, following the instrumental response of the SPAD detector. Note also that the resonant PL signal decays by two orders of magnitude in about 2.5 ns, whereas the non-res. PL takes 3.5 ns to decay by the same amount.

The continuous curve in Fig. 3 was obtained by convolution and curve fitting.[17] A function $f(t)$ given by a sum of exponentials of the form

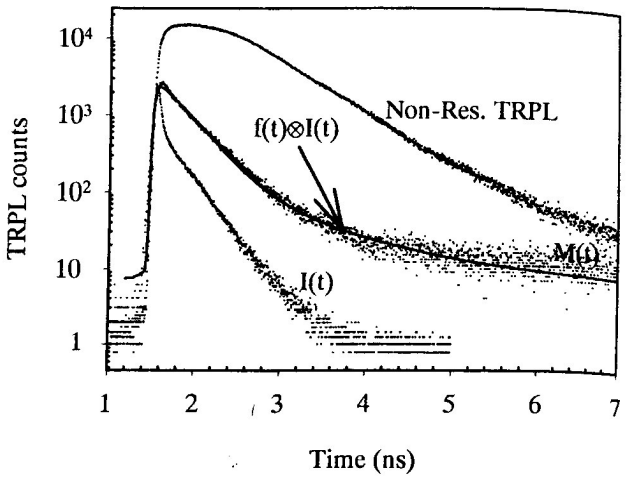

Fig. 3. Resonant excitation TRPL of the QDs, detected at 900 nm. The curves shown are the instrumental response $I(t)$, the measured PL decay $M(t)$ and the best fit $f(t) \otimes (I(t)$. The TRPL decay obtained by non-res. pumping is also shown for comparison. The acquisition times were 1200 s and 60 s respectively, for resonant and non-resonant excitation.

$$f(t) = A + \sum_{i=1}^{m} B_i e^{-t/\tau_i} \tag{1}$$

and having suitable guesses for the decay parameters τ_i and B_i was convolved with the instrumental response $I(t)$. The resulting function was then fitted by a least squares procedure to the measured TRPL decay $M(t)$. In Fig. 3, a sum of two exponentials (plus the constant background A) was used for $f(t)$. The amplitudes B_i and decay times obtained were $\tau_1 = 158$ ps, $\tau_2 = 1064$ ps, $B_1 = 0.017$ and $B_2 = 0.001$. τ_1 corresponds to the initial decay of the PL and involves only about 40 points in the curve. Also, it can be seen in the figure that, in this part of the curve, the fitting does not describe accurately the experimental results. τ_2 on the other hand, is of the order of a nanosecond and describes the time-scale over which the experimental curve decays by more than two orders of magnitude. Therefore, τ_2 is the decay time of interest, representing the dominant non-radiative recombination process for most of the carriers.

It was not possible to measure resonant PL at wavelengths shorter than 890 nm, due to the pump laser light leaking through the interference filter and overwhelming the PL signal. For wavelengths longer than 930 nm, there was not enough signal to detect a reliable TRPL decay either. This is somewhat surprising, as cw PL peaks were detected at 910, 940 and 980 nm. However, the PL signal for resonant excitation was at least 200 times lower than that for non-resonant excitation, as explained below. Note also that the cw PL peaks were obtained with a different pump wavelength and pump power and a direct comparison with the TRPL results might not be possible here. Obviously, the shape of the cw PL spectrum and the relative intensities of the peaks depend on the pump intensity, wavelength, etc. The cw PL was used only as an indication of which wavelengths should be tried in the TRPL experiments. Therefore, resonant PL was measured at only five different wavelengths and the resulting curves were analysed as above. These results will be discussed later on, in §3.

By replacing the pump laser with another one having a

much shorter wavelength, a non-resonant pumping experiment was carried out. A 677 nm (1.84 eV) semiconductor laser producing pulses of energy and width similar to the previous one was used to excite the samples. In this case, both the InGaAs quantum dots and the AlGaAs barriers are pumped and carriers generated in the barrier layers are quickly captured by the dots, before recombining. Incidentally, this pump wavelength is much closer to that used for obtaining the cw PL spectrum. Thus, carriers will be generated at a similar depth in the samples.

The non-resonant pumping experiments were also performed at 77 K and a much larger PL intensity was found, in comparison with the resonant excitation case. It is interesting to compare the PL intensity integrated over the measuring time window for the resonant and non-resonant excitation conditions. When the detection wavelength of 900 nm (same as in Fig. 3 above) was selected, it was found that the signal was 200 times larger than that obtained in the resonant pumping experiment at the same wavelength. As the PL intensity is proportional to the product np of the electron and hole concentrations, this implies that a lower (by more than one order of magnitude) carrier concentration is being generated in the resonant case. In Fig. 4 the non-resonant PL decay at the wavelength of 920 nm is presented, as well as the instrumental and the best fit curve. Despite using a different laser, the instrumental response is virtually identical to that obtained with the 870 nm laser.

The measured PL signal $M(t)$ on the other hand, is significantly different from the one obtained by resonant excitation. First of all, the PL intensity decays much more slowly. Secondly, the risetime is fast, but there is a plateau on the curve, once the maximum intensity is reached. Evidently, a more complex model of the carrier dynamics is needed to account for these features than that in eq. (1), used for the resonant pumping case. The output of the rate equation model, given by eq. (2)–(6) below, was convolved with the instrumental response and used to fit the PL decays obtained by non-resonant pumping:

$$\frac{dn_D}{dt} = R_{cn}(n_{D0} - n_D)n_B - \frac{n_D}{\tau_{rec}} \quad (2)$$

$$\frac{dp_D}{dt} = R_{cp}(p_{D0} - p_D)p_B - \frac{p_D}{\tau_{rec}} \quad (3)$$

$$\frac{dn_B}{dt} = -R_{cn}(n_{D0} - n_D)n_B \quad (4)$$

$$\frac{dp_B}{dt} = -R_{cp}(p_{D0} - p_D)p_B \quad (5)$$

In these equations, n_D, n_B, p_D and p_B are the electron and hole concentrations in the dots and in the barriers, respectively; n_{D0} and p_{D0} are the density of electron and hole states in the dots and R_{cn} and R_{cp} are the rate of capture by the dots, of electrons and holes, respectively. τ_{rec} is the (non-radiative) recombination time for electrons and holes.

The first term on the right hand side of eq. (2) gives the rate of change of the electron concentration captured by the dots, from the barriers. Note that this is a source and also a saturating term: the largest possible value of n_D is n_{D0}. The other term in eq. (2) gives the non-radiative carrier recombination and acts as a sink term. The other equations have a similar interpretation.

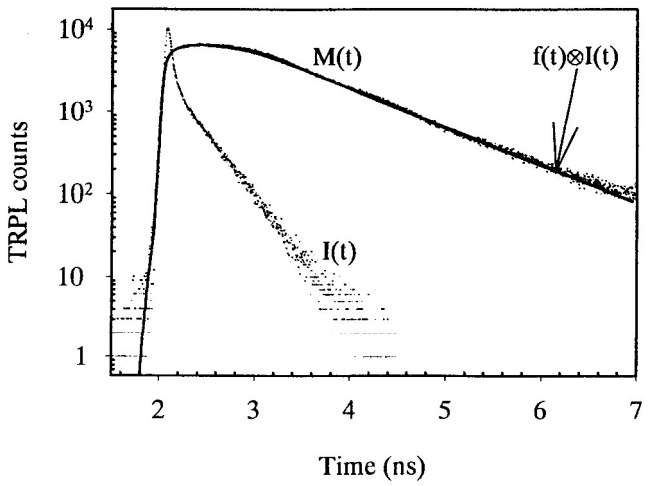

Fig. 4. Non-resonant excitation TRPL of the QDs at 920 nm. Again, the instrumental $I(t)$, the measured PL, $M(t)$ and the best fit are shown.

For the estimated carrier concentration generated in these experiments (10^{16} to 10^{17} cm^{-3}, as explained in the next section), Auger and radiative recombination are not important and can be neglected. Large scale diffusion effects can also be ruled out, due to the high density of QDs in the sample. For InGaAs or AlGaAs materials, the electron diffusion coefficient is at least $D = 5\,\text{cm}^2/\text{s}$ and so, the carrier diffusion length $L_d = [Dt]^{1/2} = 710\,\text{nm}$ for $t = 1\,\text{ns}$. As the dot separation is only 34 nm, the spatial profile of the carrier concentration is not affected by diffusion. The use of $t = 1\,\text{ns}$ above is somewhat arbitrary, but it clearly shows that, for the timescale of the PL decay in Fig. 4, diffusion out of the illuminated area will be negligible. A generation term, taking into account the temporal shape of the laser pulse, has also been neglected. The PL signal $f(t)$ is proportional to the product $n_D(t)$ and $p_D(t)$. So, neglecting a constant background and a constant multiplicative factor, the theoretical PL decay is given by:

$$f(t) = n_D(t) \cdot p_D(t) \quad (6)$$

The set of equations (2–6) above contains many approximations, but it is an improvement on models of the carrier dynamics in QDs. In general, only the simple case where the PL decay can be fitted to one or two exponentials is treated.[18]

The same process of convolution and least-squares curve fitting used before was employed here to fit the result of the convolution $f(t) \otimes I(t)$ to the measured PL, $M(t)$. In this case, eqs. (2–6) above have to be solved and a merit function $\chi(R_{cn}, R_{cp}, n_{D0}, p_{D0}$ and $\tau_{rec})$ is minimised. It was found however, that the fitting procedure often converged to local minima of $\chi(R_{cn}, R_{cp}, n_{D0}, p_{D0}$ and $\tau_{rec})$, resulting in large values of χ. In order to reduce the dimensionality of the parameter space being searched, likely ratios of p_{D0}/n_{D0} and R_{cp}/R_{cn} were selected. In typical GaAs/AlGaAs quantum wells, the number of bound (heavy) hole states is 3 to 5 times larger than the number of bound electron states. So, the ratio p_{D0}/n_{D0} is a natural number less than 5. A simple estimate of the ratio R_{cp}/R_{cn} can also be obtained as follows. The rate of capture R_c of carriers by the QD is $R_c \propto \sigma v$, where σ is the QD capture cross-section and $v = [2E/m]^{1/2}$ is the carrier velocity, E the kinetic energy and m the mass. Therefore,

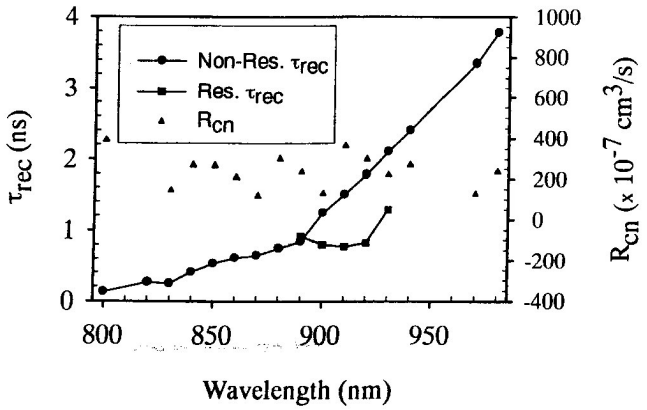

Fig. 5. Decay times τ for resonant and non-resonant excitation and the QDs electron capture cross-sections R_{cn}, as a function of wavelength.

assuming that electrons and holes have the same kinetic energy and roughly the same capture cross-section σ, their rate of capture will be given by $R_{cp}/R_{cn} = [m_e/m_h]^{1/2} \sim 1/3$. Thus, it is reasonable to constrain the two hole parameters by the equations: $p_{D0} = m \cdot n_{D0}$ and $R_{cp} = R_{cn}/m$. This reduced the number of parameters to fit to only three, not counting m, as it can be varied manually.

After testing various integer values of m, it was found that the best fits were produced for $m = 3$. With this simplifying assumption, the model could easily minimise $\chi(R_{cn}, n_{D0}, \tau_{rec})$ and the PL decays obtained for wavelengths ranging from 800 nm up to 980 nm were then analysed. The mean and standard deviation of the density of electron states in the QDs were found to be $n_{D0} = (5.5 \pm 1.1) \times 10^{17}\,\mathrm{cm}^{-3}$ and this will be compared to estimates in the next section. The values obtained for R_{cn} and τ_{rec}, for the wavelength range above have been plotted in Fig. 5. The resonant recombination times obtained previously are also plotted for comparison.

The capture cross-section R_{cn} would not be expected to be wavelength-dependent and, despite the scatter in the values found (on 14 different wavelengths), no trend is observed. The mean and standard deviation obtained were $R_{cn} = (2.5 \pm 0.9) \times 10^{-5}\,\mathrm{cm}^3/\mathrm{s}$. In the next section we discuss the results of both the resonant and non-resonant pumping experiments. The implications of these results to real laser operation will also be considered.

3. Discussions

In this section, R_{cn} and estimates for the generated carrier concentration N, are used to derive a carrier capture time τ_{cap} for non-resonant pumping. Next, an independent estimate of the 3D density of dots is made. This is used to check the value of N_{D0} produced by the rate equation model. After that, the risetimes of the TRPL obtained by resonant and non-resonant pumping schemes are discussed. Finally, the decay times of the TRPL curves are treated. A comparison with previously published results is made and the present results are shown to be in better agreement with the expected behaviour for both pumping schemes. The differences in decay times are highlighted and this is used to draw some conclusions about the carrier dynamics in VECODs.

As mentioned previously, the pumping laser pulses had an energy of 0.5 pJ, which corresponds to 2.3×10^6 photons/pulse at the wavelength of 677 nm (non-resonant excitation). If an absorption coefficient $\alpha = 10^4\,\mathrm{cm}^{-1}$ for the QD and barrier layers is assumed, then a carrier concentration $N \approx 3 \times 10^{17}\,\mathrm{cm}^{-3}$ would be generated. At this carrier concentration, the capture cross-section obtained above would result in a capture time of only $[R_{cn} \times N]^{-1} = 0.1$ ps. However, in the present QD structure, such a high carrier concentration might not have been generated, due to a lower absorption coefficient or to residual absorption in the thin (doped) layer left above the QD structures. Also, the carrier concentration generated would not be homogeneous, but decaying exponentially with the depth of the layers. It would also vary in the plane of the sample, due to the spatial profile of the laser pulse. Thus, the initial capture time would be expected to vary locally in the sample and its spatially averaged value would be somewhat uncertain. However, a conservative estimate of the average carrier concentration N_{av} is that it would be at most, one order of magnitude smaller than the local value N. This results in an average electron capture time by the QDs of $\tau_{cap} = 1$ ps. Therefore, the carrier capture observed in the present experiments is a very fast process and the plateau appearing in the PL decays obtained by non-resonant excitation comes, not from a slow carrier capture, but rather from the state filling processes occurring after capture, as modelled by eqs. (2)–(6).

The 3D density of dots can be estimated from the 2D density ($8.6 \times 10^{10}\,\mathrm{cm}^{-2}$) and the vertical dot separation of 6.2 nm. The resulting 3D density is then $1.4 \times 10^{17}\,\mathrm{cm}^{-3}$, which is about a factor of two smaller than the generated carrier concentration estimated before. Thus, on average there will be at least two electrons to be captured by each dot. This experimental estimate of the 3D QD density can also be used to check the output of the rate equation model. Three peaks were found in the cw PL of the QDs. Assuming that they come from different electron levels in the dots and using the 3D QD density above, the total density of electron states is found to be $4.2 \times 10^{17}\,\mathrm{cm}^{-3}$. This is close to the value of n_{D0} produced by the rate equation model ($n_{D0} = 5.5 \times 10^{17}\,\mathrm{cm}^{-3}$), although the model seems to imply the existence of 4 energy levels in the QDs. In view of all the uncertainties in these parameters, this result is considered to be satisfactory.

Next, the resonant and non-resonant pumping experiments are compared in terms of PL risetimes and with previously published experiments. It was seen in Figs. 3 and 5 that the PL risetime is very fast for both pumping schemes. These results are in direct contradiction to those presented in ref. 19, where a 400 ps risetime was found for resonant pumping. This long and constant (wavelength independent) risetime was interpreted as evidence of a phonon bottleneck effect. In that study it was found, in addition, that both the rise and decay of the TRPL were larger for resonant than for non-resonant excitation. This behaviour is completely different from the known results in quantum wells. In 2D systems, the risetime is shortened when one goes from non-resonant to resonant excitation.[20] The situation should not be different in 3D systems like the VECODs. When carriers are generated in the AlGaAs barriers (non-resonant case), they will take time to be captured by the QDs. In resonant pumping, the carriers are generated already in the dots and a capture and local-diffusion time does not contribute to increase the risetime of the PL signal. Therefore, the PL risetime for resonant pumping should

be shorter than or as short as that for the non-resonant case. This is precisely what was found in the present study.

The resonant PL risetime is very fast (Fig. 3) and follows the instrumental response of the system. Thus, it is shorter (probably by more than one order of magnitude) than the risetime (10–90%) of the instrumental response, which is about 50 ps. Therefore, the phonon bottleneck for carrier relaxation can be ruled out in these samples. It is interesting to contrast this value with that of ref. 19, where a 400 ps risetime was obtained. Independent measurements of the PL risetime in quantum dots also produced a value close to that of the excitation pulse.[21]

For the non-resonant risetime on the other hand, the carrier capture cross-section was combined before, with reasonable estimates of the photocarrier concentration to produce a risetime of about 1 ps. Therefore, the risetimes for the two pumping schemes should be of the same order of magnitude.

There has been some speculation that carrier capture by the QDs could be very slow (due to the complicated carrier dynamics once some of them are captured) and this would be detrimental to the operation of lasers based on these structures. The results above show that VECODs can capture the carriers generated in the barriers very efficiently, at least for carrier concentrations up to $3 \times 10^{17}\,\mathrm{cm}^{-3}$.

So far, only the risetimes have been discussed. Now the PL decays for resonant pumping will be considered. As seen in Fig. 3, the PL decay for resonant pumping was fast, with a time constant obtained at 900 nm wavelength of $\tau_2 = 0.8$ ns. Similar decay times, but slightly increasing, were obtained at longer wavelengths. These results were presented together with those for non-resonant pumping in Fig. 5, which also shows that the resonant decay times are always shorter than the non-resonant, which is to be expected.

A very small carrier concentration was generated in the resonant pumping case, as evidenced by the fact that the PL signal was much smaller (by a factor of 200) than in the non-resonant case. Therefore, the resonant PL decay times can be taken as a measure of the intrinsic decay times of the quantum dots, unaffected by carrier capture, band filling and other effects. In particular, the intrinsic lifetime measured at 930 nm is 1.3 ns. The shorter decay times obtained for shorter wavelengths is consistent with carrier depletion, due to relaxation, of the excited states into the ground state. Again, this seems to rule out a phonon bottleneck in these experiments, since that effect would produce a longer decay time for shorter wavelengths.

It should be emphasised that the material studied here has ten layers of vertically coupled quantum dots. This could have an effect on the carrier dynamics, with carriers transferring from smaller dots (higher energy levels) to larger and unoccupied ones, in deeper layers. This would further complicate the carrier dynamics and might even prevent a phonon bottleneck effect from taking place. Ideally, time-resolved intraband absorption measurements between electron levels in (doped) QDs should be performed, using perhaps a free-electron laser in a pump-probe set-up.[22] This could produce an independent confirmation of the results above, regarding the absence of a phonon bottleneck effect in these structures.

The non-resonant PL decay times are discussed now and compared with the resonant case. Due to the much larger PL signal in non-resonant pumping, it was possible to measure the decay times at 15 different wavelengths. It was found that the non-resonant decay time increased rapidly with the wavelength, as shown in Fig. 5. This is due to a combination of PL from more than one level being detected at a single wavelength, as the three VECOD energy levels overlap to a great extent. Thus, as the detection wavelength increases from 910 to 940 nm for example, the contribution to the detected PL coming from the 910 peak is decreasing, while that originating from the 940 nm peak is increasing. This results in a smooth transition from the decay time from one energy level to the next being observed.

Another interesting feature of the results in Fig. 5 is the large difference in decay times for resonant and non-resonant pumping. If the wavelength of 890 nm is selected, then the two decay times are virtually identical, being 0.85 ns. As the wavelength increases, the non-resonant decay time increases rapidly and at 930 nm, their *difference* is $\Delta t = 820$ ps. This can be attributed to a slowing down of carrier relaxation caused by state filling, as the phonon bottleneck effect was ruled out by the resonant pumping experiment. If the ground state and lower excited states of the dots were empty, the decay time should not depend on which pumping scheme created the carriers. However, in the non-resonant case, a much larger carrier concentration results, which can produce a state filling effect similar to band filling in quantum wells.[7] In this case, it should take longer for the carriers to decay, due to the unavailability of empty states. This is what was observed in Fig. 5; the lower the state, the longer it takes for it to finally empty. Thus state filling gives a density-dependent bottleneck.

4. Conclusion

The relaxation mechanisms of an array of 10 stacked layers of vertically coupled quantum dots have been studied. Both resonant and non-resonant excitation were employed to create the photocarriers. It was found in the non-resonant pumping experiment, that the carrier capture by the QDs is a very fast process, being of the order of 1 ps. In the resonant case, the PL risetime is also very fast, following the risetime of the instrumental response. Therefore, a phonon bottleneck effect for carrier relaxation does not seem to be present in these samples.

The decay times at a given wavelength are always shorter for resonant than for non-resonant excitation. In addition, the difference between these decay times increases rapidly with wavelength. This is interpreted in terms of the carrier concentrations generated by both pumping schemes. For non-resonant excitation, a much larger carrier concentration is produced. Due to the relatively small density of states, carrier relaxation is slowed down in this case, by a state filling effect.

A variety of mechanisms can influence the carrier dynamics in QD systems, before and after carrier capture. It is likely that QDs made of different materials or having different layer compositions, will not share the same set of relaxation mechanisms or at least, the dominant mechanism might be material-dependent. In addition, it is likely that samples with many layers of vertically coupled QDs might possess even more complicated relaxation paths.

Acknowledgements

The Q-switched laser diodes used in this work were sup-

plied by E. L. Portnoi and co-workers, A. F. Ioffe Institute, St. Petersburg, Russia. The actively quenched SPADs are used by agreement of S. Cova and co-workers, Polytechnico di Milano, Italy.

1) C. Guasch, J. Ahopelto, H. Lipsanen, M. Sopanen, C. M. Sotomayor Torres, I. Gontijo and G. S. Buller: Inst. Phys. Conf. Ser. **155** (1996) 813.
2) H. Benisty, C. M. Sotomayor-Torres and C. Weisbuch: Phys. Rev. B **44** (1991) 10945.
3) T. Inoshita and H. Sakaki: Phys. Rev. B **46** (1992) 7260.
4) U. Bockelmann and T. Egeler: Phys. Rev. B **46** (1992) 15574.
5) Al. L. Efros, V. A. Kharchenko and M. Rosen: Solid State Commun. **93** (1995) 281.
6) S. Raymond, S. Fafard, P. J. Poole, A. Wojs, P Hawrylak, S. Charbonneau, D. Leonard, R. Leon, P. M. Petroff and J. L. Merz: Phys. Rev. B **54** (1996) 11548.
7) I. Gontijo, G. Tessier, M. Livingstone, I. Galbraith and A. C. Walker: J. Appl. Phys. **80** (1996) 4027.
8) K. Mukai, N. Ohtsuka, H. Shoji and M. Sugawara: Phys. Rev. B **54** (1996) 5243.
9) K. H. Schmidt, G. Medeiros-Ribeiro, M. Oestreich and P. M. Petroff: Phys. Rev. B **54** (1996) 11346.
10) V. M. Ustinov, A. Yu. Egorov, A. R. Kovsh, A. E. Zhukov, M. V. Maximov, A. F. Tsatsul'nikov, N. Yu. Gordeev, S. V. Zaitsev, Yu. M. Shernyakov, N. A. Bert, P. S. Kop'ev, Zh. I. Alferov, N. N. Ledentsov, J. Bohrer, D. Bimberg, A. O. Kosogov, P. Werner and U. Gosele: J. Cryst. Growth **175/176** (1997) 689.
11) S. Zaitsev, N. Yu. Gordeev, Yu. M. Sherniakov, V. M. Ustinov, A. E. Zhukov, A. Yu. Egorov, M. V. Maximov, P. S. Kpo'ev, Zh. I. Alferov, N. N. Ledentsov, N. Kirstaedter and D. Bimberg: submitted to Superlatt. & Microstruct.
12) A. O.Kosogov, P. Werner, U. Gosele, N. N. Ledentsov, D. Bimberg, V. M. Ustinov, A. Yu. Egorov, A. E. Zhukov, P. S. Kop'ev and Zh. I. Alferov: Appl. Phys. Lett. **69** (1996) 3072.
13) G. S. Buller, J. S. Massa and A. C. Walker: Rev. Sci. Instrum. **63** (1992) 2994.
14) S. Cova, M. Ghioni, A. Lacaita, C. Samori and F. Zappa: Appl. Opt. **35** (1996) 1956.
15) A. Lacaita, M. Ghioni and S. Cova: Electron. Lett. **25** (1989) 841.
16) S. Cova, A. Lacaita, M. Ghioni, G. Ripamonti and T. A. Louis: Rev. Sci. Intrum. **60**(1989) 1104.
17) D. V. O'Connor and D. Phillips: *Time-correlated Single Photon Counting* (Academic Press, New York, 1983).
18) R. Heitz, A. Kalburge, Q. Xie, M. Grundmann, P. Chen, A. Hoffmann, A. Madhukar and D. Bimberg: Phys. Rev. B **57** (1998) 9050.
19) F. Adler, M. Geiger, A. Bauknecht, F. Scholz, H. Schweizer, M. H. Pilkuhn, B. Ohnesorger and A. Forchel: J. Appl. Phys. **80** (1996) 4019.
20) P. W. M. Blom, C. Smit, J. E. M. Haverkort and J. H. Wolter: Phys. Rev. B **47** (1993) 2073.
21) D. Bimberg, N. Kirstaedter, N. N. Ledentsov, Zh. I Alferov, P. S. Kop'ev and V. M. Ustinov: IEEE J. Select. Top. Quantum Electron. **3** (1997) 196.
22) B. N. Murdin, W. Heiss, C. J. G. M. Langerak, S. C. Lee, I. Galbraith, G. Strasser, E. Gornik, M. Helm and C. R. Pidgeon: Phys. Rev. B **55** (1997) 5171.